Static Axial Reciprocal Load Test of Soil-Cement Mixing Pile Applying as Permanent Pile

Koji WATANABE [i], Koji WADA [ii] and Tomoshi YOKOYAMA [iii]

i) Associate Professor, Department of Civil Engineering, Aichi Institute of Technology, 1247 Yachigusa, Yakusa Cho, Toyota, Aichi 470-0392, Japan.

ii) Deputy Manager, Construction Technological Development Department, Construction Robotics Division, Obayashi Corporation, Shinagawa Interecity Tower B, 2-15-2, Konan, Minato-ku, Tokyo 108-8502, Japan.

iii) General Manager, Procurement Management Department, Obayashi Corporation, Shinagawa Interecity Tower B, 2-15-2, Konan, Minato-ku, Tokyo 108-8502, Japan.

ABSTRACT

The soil-cement mixing wall has previously been used as an earth retaining wall during excavations, and was treated as a temporary structure. At present, a method has not been established for evaluating its assumed vertical bearing capacity and tensile resistance when bearing a building body load or something similar. In recent years, rationalization of the foundation structure, reduction of the environmental burden, and other needs have been rising, studies have been proceeding into the application of soil-cement mixing walls as permanent piles. In addition, with the previously temporary soil-cement mixing wall now being used as a permanent pile, it can be expected that eliminating the need for new work and reduce construction expenses. This study aimed for the application of the embedded portion of soil-cement mixing wall as a permanent pile, and evaluated the magnitude of the bearing capacity and the tensile resistance for assuming the failure between ground and pile in the static axial reciprocal load test for single soil-cement mixing pile.

Keywords: soil-cement mixing wall, static reciprocal load test, single pile, shaft friction, end bearing capacity

1 INTRODUCTION

An examination was performed on the use of soil-cement mixing walls, which have been treated previously as temporary structures left buried in the ground, as permanent piles in order to rationalize foundation structures and to reduce environmental burdens (Fig. 1). The core materials of such walls, which are used as the foundation pile and whose embedded portions act as a permanent pile, comprise the stress-transmitting member in the soil-cement column. The construction machinery used to build temporary structures using such walls was used to construct the soil-cement mixing wall in this study, and the range for the strength of the soil-cement was assumed to be in the commonly adopted range (500 to 2000kN/m^2). The vertical bearing capacity of the soil-cement mixing wall where the embedded portion is used as a permanent pile was examined by hypothesizing two types of failure modes: failure of the ground and sliding failure between the soil-cement and the H-shaped steel surface.

There are some previous researches on the use of soil-cement mixing wall as a permanent pile. Watanabe et al. (2013) carried out in-situ full scale load test to confirm the bearing capacity of soil-cement mixing pile. They reported that the bearing capacity of soil-cement mixing pile is equivalent to the bearing capacity of a cast-in-place concrete pile. Moreover, it is important to obtain the bearing properties of pile body because the failure of pile body is considered such as bond failure between soil-cement and surface of H-shaped pile, and compression failure at pile tip between H-shaped pile and soil-cement. Mizumoto et al. (2013) were carried out the model load test to confirm the load transfer mechanism of pile body on soil-cement mixing pile. They examined the stud effect and the effect of confining pressure acting to the pile body. The bond strength between soil-cement and surface of H-shaped pile was reported by Watanabe et al. (2014). They concluded that the peak bond strength is estimated by 11~21% of

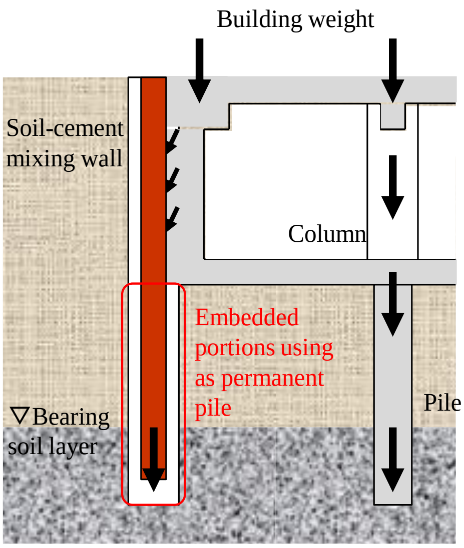

Fig. 1. Schematic view of soil-cement mixing wall using permanent pile.

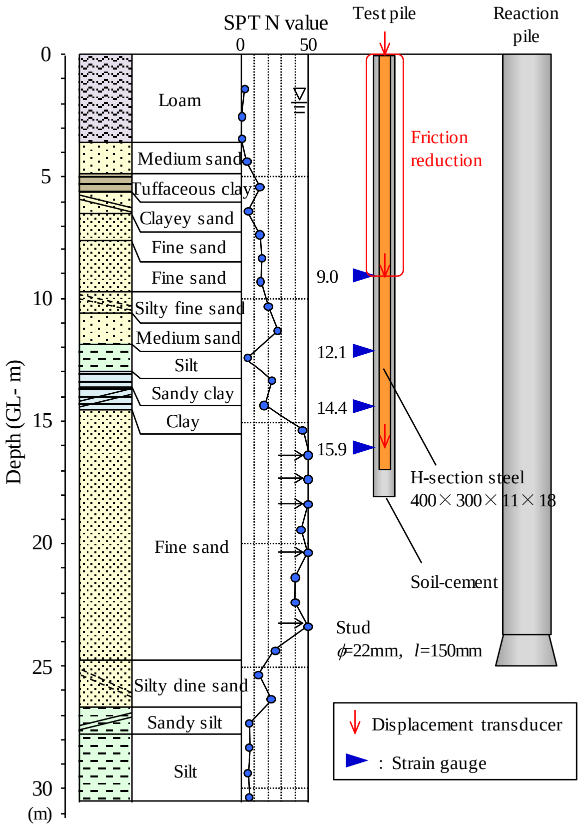

Fig. 2. Test pile and ground condition (Site A).

unconfined compressive strength and the residual bond strength is estimated by 3% of unconfined compressive strength. From these study, the load transfer mechanism from the H-shaped steel, which acted as the stress-transmitting member, to the soil cement had to be examined.

This study aimed for the use of the embedded portion of such a structure as a permanent pile, and evaluated the magnitude of the shaft friction and the magnitude of the

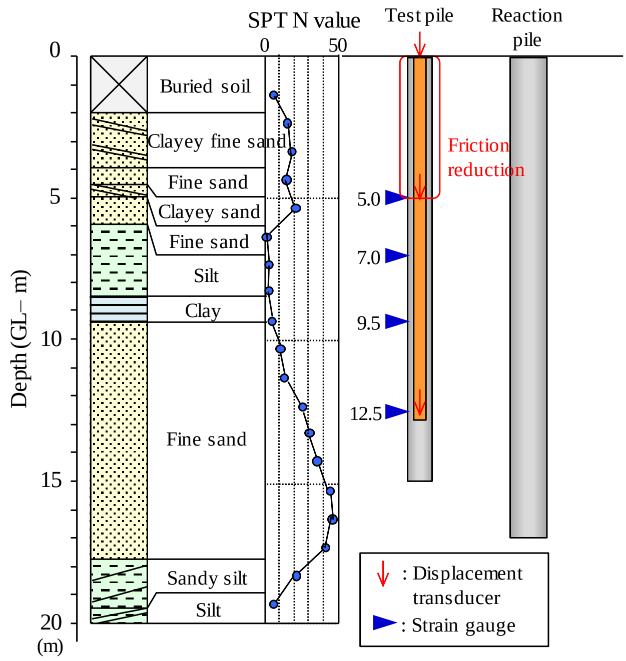

Fig. 3. Test pile and ground condition (Site B).

Table 1. Specifications of test piles.

Site	Pile diameter (mm)	Pile length (m)	Length of H-section steel (m)	Strength of soil-cement (kN/m^2)	Stud
Site A	600	18.0	17.0	500	With stud
Site B	600	15.0	13.0	500	With stud

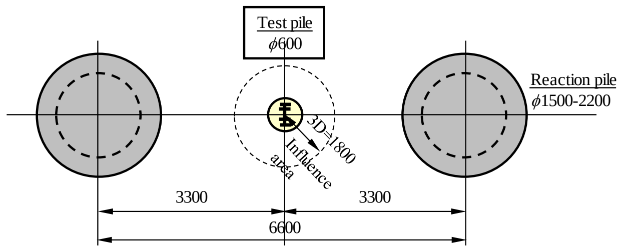

(a) Site A.

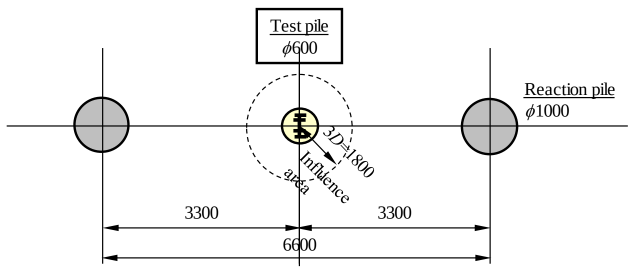

(b) Site B.

Fig. 4. Arrangement of Test piles and reaction piles.

bearing capacity in a full-scale load test. This paper firstly describes the background and the previous study, secondly indicates the load test, then presents the results of full-scale load test, and finally discusses the evaluation of pile resistance on soil-cement mixing pile.

2 STATIC AXIAL RECIPROCAL LOAD TEST

The ground conditions and test piles for Site A and Site B are described in Fig. 2 and Fig. 3 respectively. The test ground of Site A was comprised of loam soil and tuffaceous clay approximately GL -5.5m, and comprised primarily with fine-grain and medium-grain sand at depths of GL -12.0m, then comprised of silt and clay at approximately 15.0m, and comprised of fine sand at deeper depth. In Site B, the ground was comprised of fine sand and clayey sand up to GL-6.5m, and comprised with silt and clay at approximately 7.0m, then comprised of fine sand at deeper depth. Static axial reciprocal load test was carried out in two site called as Site A and Site B. The specifications for the test piles are listed in Table 1. The test piles were embedded in the ground with the pile tip driven into the ground to an N value of approximately 50 and 30 for Site A and Site B, respectively. Furthermore, a diameter of 600mm was adopted for both Site A and Site B of the soil-cement improving body diameter (pile diameter) of the test piles, while dimensions of H-400×300×11×18 were adopted for the H-section steel.

The design strength of the soil-cement improving body was 500kN/m^2. The strength of the soil-cement improving body was confirmed to satisfy the design strength of 500kN/m^2 based on the results from an unconfined compression test performed after the load test had been completed, on specimens with their cores extracted.

The arrangements of test piles and reaction piles are shown in Figure 4. Test piles were arranged between for reaction piles, out of consideration for their influence range as described in the Japanese Geotechnical Society ("Methods for vertical load test of piles") (2001), the distance are 3*D*=1800 (mm). Here, *D* means the pile diameter such as the soil cement diameter.

The load test was performed in compliance with the standard of the Japanese Geotechnical Society entitled Method for Vertical Load Test (2002). Stepwise loading and the multiple-cycle method were adopted as loading methods. The duration of the new loading step was set to 30min, while the duration of the historical loading step was set to 2min and the duration of the zero-loading step was set to 15min.

The measurement items consisted of the load and displacement of the pile top as well as the strain of the H-section steel. The measurements of the displacements at pile tip were taken using the double-pipe method. Here, the strain of H-section steel was measured at the pile head, the pile tip and the boundary of each soil stratum.

4 RESULTS OF FULL-SCALE LOAD TESTS

4.1 Site A

Figure 5 shows the relationships between the load and displacement at the pile head. The maximum loads

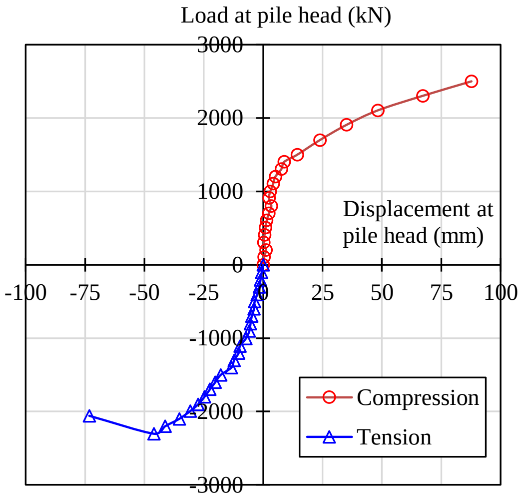

Fig. 5. Relationship between load and displacement at pile head (Site A).

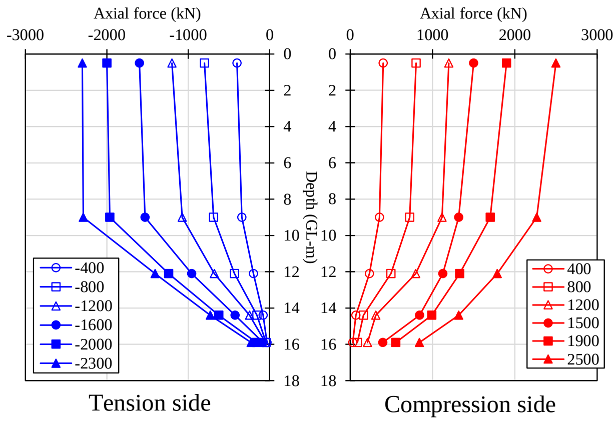

Fig. 6. Axial force distribution (Site A).

were 2500kN for compression loading and -2200kN for tension loading. For all loading, the curve was steep from the initial of loading; all of the piles possessed a large initial stiffness. The gradient of the curve then changed with the loading and reached the maximum load.

The axial force was calculated by considering only the H section steel. The strain of the H section steel obtained from the load test was multiplied with the Young's modulus and cross-sectional area of the H section steel. The distributions of axial force both compression side and tension side present in Fig. 6. It is said that the shaft resistance mobilizes at each section because the difference of axial force at each section is large as the applied load increases. It is also pointed out that the pile tip resistance increases because the axial force at the pile tip shows the large value when the applied load increases. The relationships between the shaft friction and local pile displacement which was obtained by dividing this axial force difference by the circumferential area are shown in Fig. 7. The improved diameter of the soil cement (i.e. outer diameter of soil cement column) was used when calculating the

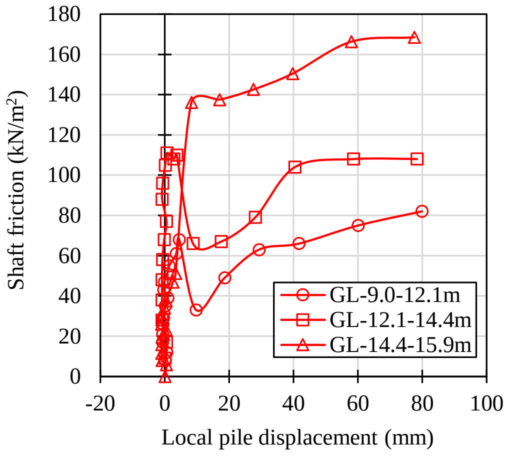

(a) Compression side.

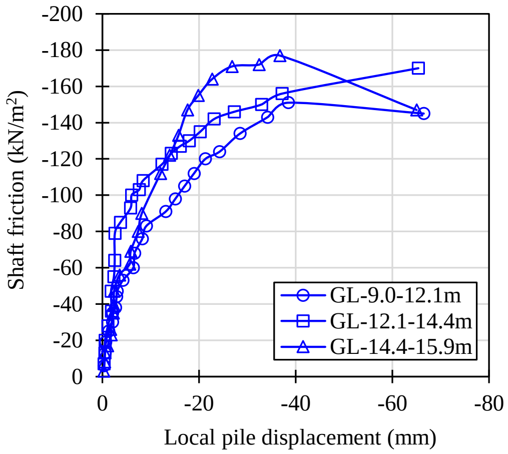

(a) Tension side.

Fig. 7. Relationships between shaft friction and local pile displacement (Site A).

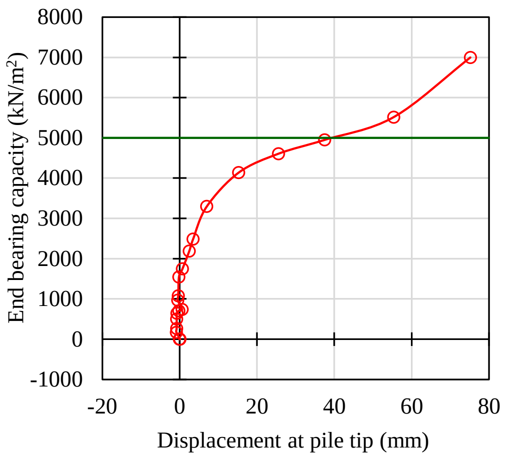

Fig. 8. Relationship between end bearing capacity and displacement at pile tip (Site A).

circumferential area of the pile. Figure 7(a) shows that a maximum shaft friction of 80 ~ 170kN/m^2 was reached in the compression side. In the tension side, it is observed that the maximum shaft friction is 150~180kN/m^2. Therefore, it is said that the shaft friction of the tension

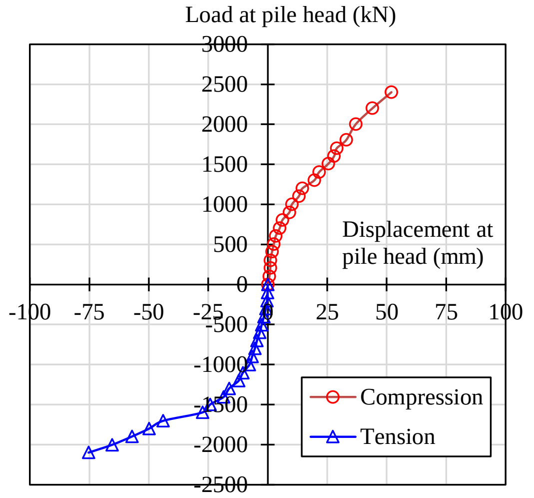

Fig. 9. Relationship between load and displacement at pile head (Site B).

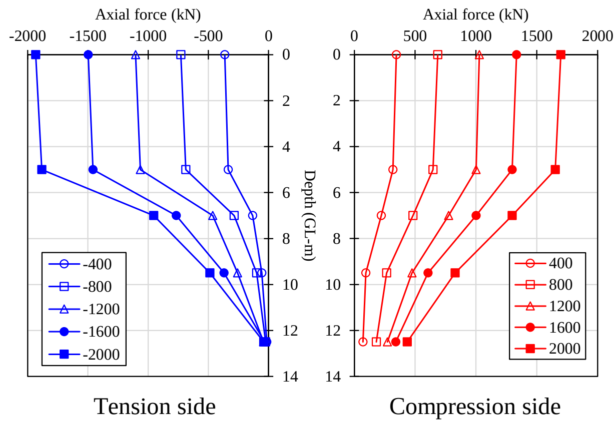

Fig. 10. Axial force distribution (Site B).

side is larger than that of the compression side.

The end bearing capacity was calculated by dividing the axial force reaching the pile tip by the envelope area of the H-section steel (*B*x*H*). The relationship between the end bearing capacity and displacement at pile tip indicates in Fig. 8. The reference displacement of pile tip is 10% of the diameter of the equivalent circle area which is equal to the envelope area of H-section steel pile when the end bearing capacity is evaluated. The end capacity of 5500kN/m^2 is examined in this load test. The trend indicates that the end bearing capacity is gradually increasing as the displacement at pile tip increases.

4.2 Site B

The relationships between the load and displacement at the pile head is shown in Fig. 9. The maximum loads were 2400kN for compression loading and -2100kN for tension loading. For all loading, the curve was steep from the initial of loading, and the gradient of the curve then changed before the loading was reached the maximum load in the tension loading.

The distributions of axial force both compression side and tension side present in Fig. 10. Here, the axial force is estimated by the same method as described in the

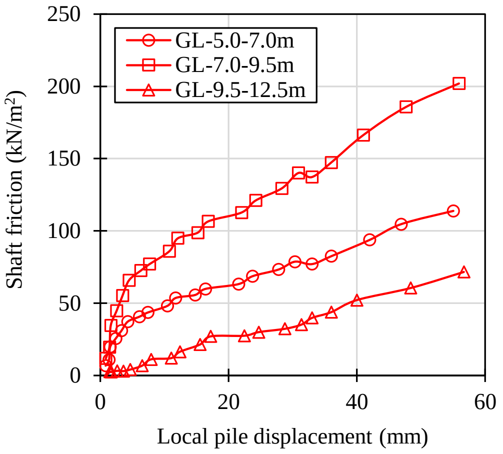

(a) Compression side.

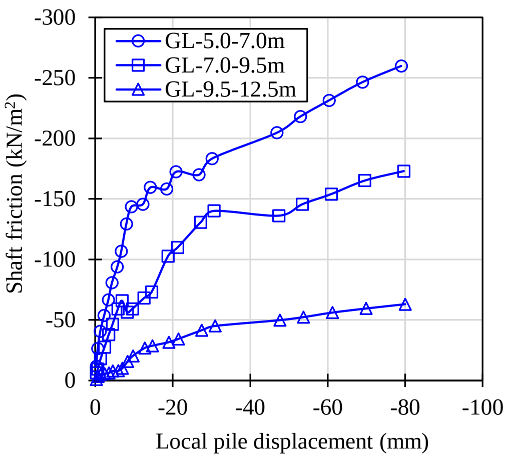

(a) Tension side.

Fig. 11. Relationships between shaft friction and local pile displacement (Site B).

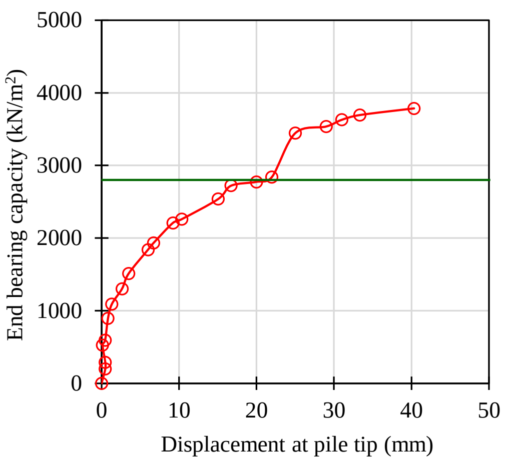

Fig. 12. Relationship between end bearing capacity and displacement at pile tip (Site B).

section 4.1. It is pointed out that the shaft resistance mobilizes at each section because the difference of axial force at each section is large as the applied load increases. It is also implied that the pile tip resistance increases when the applied load increases.

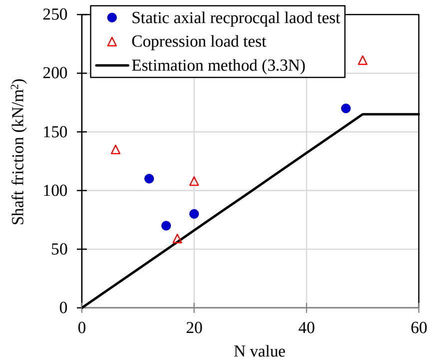

(a) Sandy soil.

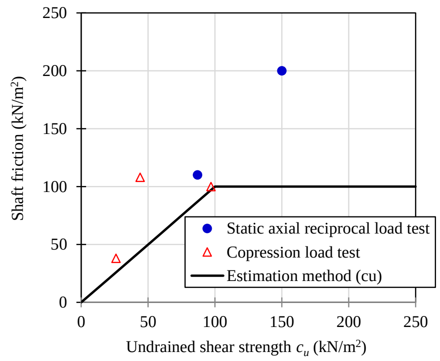

(b) Clayey soil.

Fig. 13.Comparison of shaft friction in compression side.

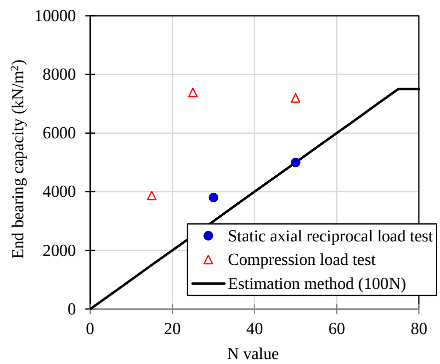

Fig. 14.Comparison of end bearing capacity.

The relationships between the shaft friction and local pile displacement are shown in Fig. 11. The estimation method of shaft friction is the same method as described in section 4.1. Figure 11(a) shows that a maximum shaft friction of 70~200kN/m^2 was reached in the compression side. According to Fig. 11(b), it is observed that the maximum shaft friction is 60~260kN/m^2. Thus, it is said that the shaft friction of the tension side is larger than that of the compression side.

The relationship between the end bearing capacity and displacement at pile tip indicates in Fig. 12. The end bearing capacity was calculated by dividing the axial force reaching the pile tip by the envelope area of the H-section steel (BxH). The reference displacement of pile tip is 10% of the diameter of the equivalent circle area which is equal to the envelope area of H-section steel pile when the end bearing capacity is evaluated. The end capacity of 3600kN/m^2 is examined in this load test.

4.3 Estimation of bearing capacity

The estimation method of bearing capacity for soil-cement mixing wall utilizing a permanent pile was developed based on static compression and tension load test. The shaft friction is estimated by Eq. (1) and Eq. (2).

For sandy soil: $\tau_S = 3.3N$ (1)

For clayey soil: $\tau_C = c_u$ (2)

Eq. (3) presents the estimation method of end bearing capacity.

For sandy soil: $p_b = 100N$ (3)

Where,

τ_s and τ_c: Shaft friction (kN/m^2)

N: N value from standard penetration test

c_u: Undrained shear strength (kN/m^2)

The relationships between shaft friction and SPT N value or undrained shear strength in the compression loading are shown in Fig. 12. From Fig. 12, the shaft friction which was obtained from the static axial reciprocal load test exceeds the estimated shaft friction. Figure 13 indicates the relationships between end bearing capacity and SPT N value. According to Fig. 13, it is said that the end bearing capacity from the static axial reciprocal load tests is larger than the estimated end bearing capacity.

The relationships between shaft friction and SPT N value or undrained shear strength in the tension loading are presented in Fig. 14. Compared to the observed shaft friction of static axial reciprocal load test and the estimated value, the observed shaft friction is larger than the estimated shaft friction.

It is said that the shaft friction for a sandy soil and a clayey soil can be estimated by Eq. (1) and Eq. (2) when the reciprocal load is applied to the soil-cement mixing wall foundation. Moreover, it can be also concluded that the end bearing capacity for a sandy soil can be estimated by Eq. (3) as the reciprocal load is applied to the soil-cement mixing wall foundation.

5 CONCLUSIONS

The purpose of this study is to examine the bearing capacity and the tension resistance for the soil-cement mixing pile in the static axial reciprocal load test, and to confirm the estimation method which was developed based on the compression and tension load tests. The following findings were obtained from this study.

1) It is said that the shaft friction for a sandy soil and a clayey soil from the static axial reciprocal load tests is larger than the estimated value.

2) It can be concluded that the end bearing capacity for a sandy soil shows the large value compared to the estimated value.

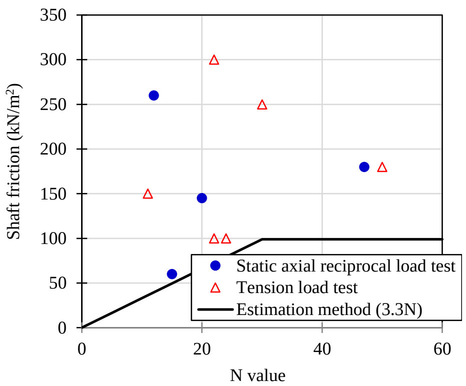

(a) Sandy soil.

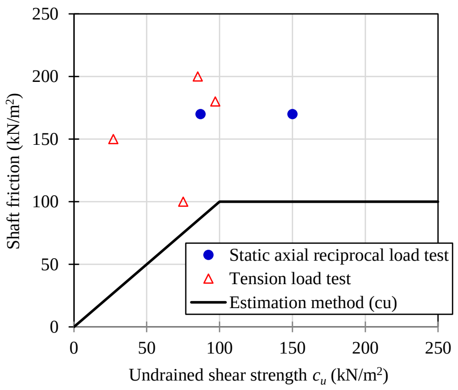

(b) Clayey soil.

Fig. 14.Comparison of shaft friction in tension side.

3) The bearing capacity and the tension resistance when the reciprocal load is applied to the soil-cement mixing wall foundation can be evaluated by the developed estimation method based on the compression and tension load tests.

REFERENCES

1) Watanabe, K. (2013): In-situ Full Scale Load Test of Soil-Cement Mixing Wall (Part 1 and 2), *Proceedings of Annual Conference of Architecture Institute of Japan*, 487-490 (in Japanese).

2) Mizumoto, M. and watanabe, K. (2013): Model Load Test of Soil-cement Mixing Wall on Load Transfer Mechanism, *Proceedings of Annual Conference of Architecture Institute of Japan*, 491-492 (in Japanese).

3) Watanabe, K. (2014): A Study on Bond Behavior of Soil Cement Mixing Wall Using Permanent Piles, *Proceedings of Annual Conference of Architecture Institute of Japan,* 495-496 (in Japanese).

4) The Japanese Geotechnical Society (2002): JGS Standard "Method for Vertical Load Test".